GenRiver input parameters

Table 2.2. The model input is thus driven by the following parameters

Acronym	Definition	Dimension [default value]	Notes
DailyRain (I,t)	Daily rainfall for each unit i	mm (= l per m^2)	Located in Stella
RainIntensMean	Average rainfall intensity	mm/day	Located in Stella
UseSpatVarRain	Option to use spatial rainfall distribution generated from SpatRain module	mm	Located in Stella
RainIntensCoefVar	Coefficient of variation of rainfall intensity		Located in Stella
DebitData	Daily discharge data	mm	Located in Stella
InterceptPerClass (j)	Interception storage capacity per land cover class	mm	Located in Excel
LandCoverFreq (i,t)	Land cover class frequency per unit i	[]	Located in Excel
MaxInfRate (i)	Maximum infiltration capacity per unit i	mm day^{-1} (500)	Located in Stella
RelativeDrought Threshold (j)	Drought-limitation to transpiration per land cover class, as fraction of field capacity	[]	Located in Excel
FieldCapacity (i)	Field capacity of the soil (soil water content 1 day after 'soaking' rain	mm (600)	Located in Stella
SoilSatminusFC (i)	Difference between saturation water storage capacity and field capacity of the soil	mm (100)	Located in Stella
MaxDynGrWatStore (i)	Dynamic groundwater storage capacity	mm (350)	Located in Stella
Routing Distance (i)	Distance from centre of subcatchment to measurement point	km	Located in Excel
PerFracMultiplier	Daily soil water drainage as fraction of groundwater release fraction	[] (0.5)	Located in Stella Located in Stella
GWReleaseFracVar	An option to have a constant groundwater release fraction for each subcatchment or using single value for the whole catchment	[] (1)	
GWReleaseFracConst (i)	Daily groundwater release fraction	[] (0.03)	Located in Stella
InitRelSoil	Initial soil water content relative to field capacity	[] (1)	Located in Stella
InitRelGroundwater	Initial groundwater store relative to maximum value	[] (1)	Located in Stella
EPot (t)	Potential evapotranspiration (Penmann type)	mm (5)	Located in Excel
Area (i)	Area of each subcatchment	km^2	Located in Excel

Note: index **t** refers to time dependent input, **i** to subcatchment and **j** to land cover classes

In the model a number of 'array' dimensions is used. Space-related properties are described with the 'sub-catchment' array, that is (potentially) used to specify soil and groundwater properties as well as the 'routing' time for stream discharge to reach the point where the river is monitored. A number of land cover classes can be distinguished (as in the 'FALLOW' model, but the GenRiver model operates on daily time steps, while FALLOW has a yearly time step), with different properties for interception of rainfall and water use by transpiration (both at the potential level and where a drought threshold is passed). Time is the main dimension of change, of course, and rainfall is the main time-dependent input, that can be made specific to each sub-catchment (but not differentiating land cover classes). Surface infiltration properties are currently described as a constant, but they may well have to be made dependent on sub-catchment. A relationship between this property and the land cover class is required that describes the change in this property as a function of time since land cover change.

2.2.5 SpatRain

Variations in river discharge tend to decrease with increasing area of consideration, partly due to a decrease in temporal correlation of rainfall events across space. Patchiness of rainfall can contribute to an increase of yield stability over space. Existing rainfall simulators tend to focus on station-level time series, not on space/time autocorrelation. The SpatRain model described here was constructed to generate time series of rainfall that are fully compatible with existing station-level records of daily rainfall, but yet can represent substantially different degrees of spatial autocorrelation. Calculations start from the assumed spatial characteristics of a single rainstorm pathway, with a trajectory for the core area of the highest intensity and a decrease of rainfall intensity with increasing distance from this core. The model can derive daily amounts of rainfall for a grid of observation points by considering the possibility of multiple storm events per day, but not exceeding the long-term maximum of observed station-level rainfall. Options exist for including elevational effects on rainfall amount. SpatRain is implemented as an Excel workbook with macros that analyze semi-variance as a function of increasing distance between observation points, as a way to characterize the resulting rainfall patterns accumulated over specified lengths of time (day, week, month, year).

The SpatRain model starts from the spatial characteristics of a single rainstorm pathway (with a trajectory for the core area of the highest intensity and a decrease of rainfall intensity with increasing distance from this core) and can derive daily amounts of rainfall for a grid of observation points by considering the possibility of multiple storm events per day. Design features include:

➢ the simulated rainfall for any point in the landscape must be consistent with existing data on the frequency distribution of daily rainfall;
➢ the program must allow for spatial trends in mean rainfall, *e.g.* due to elevational effects;
➢ the program should analyze semivariance as a function of increasing distance between observation points, as a way to characterize the resulting rainfall patterns accumulated over specified lengths of time (day, week, month, year) and identify the storm-level parameters that lead to specified degrees of spatial correlation; and

➤ for use in combination with a hydrological model, SpatRain should allow for the identification of subcatchments in a watershed area and allow averaging the point grid pattern to derive the daily average rainfall per subcatchment.

Description of the model

Approach to the problem

Station-level daily records are often the only information available on the distribution of rainfall. Such data can be represented as a series of monthly 'exceedance' graphs, derived from say 30-year data. Between months of the year and locations we may expect differences in the intercept with the X-axis or 'frequency of wet days' (or days with a measurable amount of precipitation, usually defined as > 0.5 mm day^{-1}), the intercept with the Y-axis or maximum amount of rainfall in a single day recorded in that particular month of the year, and in the curvature of the (monotonously rising) line between these two points (Fig. 2.42).
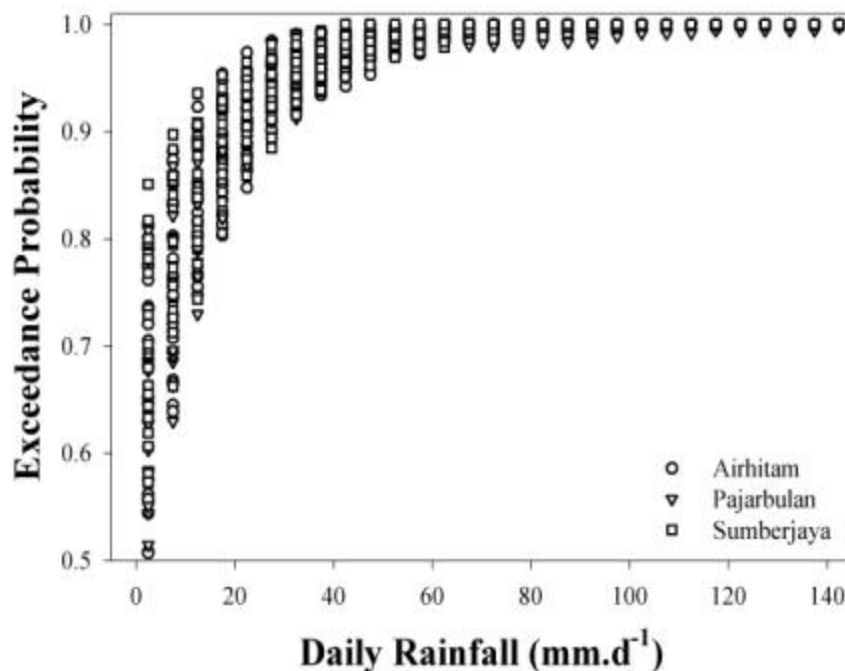

Figure 2.42. Input distribution of station level rainfall depth in three measurement stations that were combined, as they don't show essential differences.

Conceptually one can imagine a procedure that reshuffles measured daily sequences of rainfall while maintaining the monthly total, like rearranging a jackpot, where the variability of 3 values exposed on the window should follow our expectation: homogenous (apple-apple-apple) or heterogeneous (apple-banana-orange). The total set of permutations of 30 sets of jackpot with 30 pictures (for 30 days and only 30 cells) is enormous, and among these we can expect to find a substantial variation in degrees of spatial autocorrelation. By generating a sample of these reshuffling results, calculating autocorrelation and then selecting specific configurations, we would meet the key design

criteria specified above. The program will, however, be rather cumbersome and time consuming if large areas are to be considered, and the selection of results that meet a specific change in spatial autocorrelation with increasing distance may require a large subset of reshuffling results. More efficient algorithms are desirable, but the 'jackpot' analogue shows that the design rules are not mutually incompatible. A more direct approach can be taken if we assign specific spatial properties to single storm events and then adjust the frequency of storms and the intensity of rainfall in the core area of these storms to match the existing station records.

Assumed storm properties

Three parameters are used here for describing rainfall in the core area: the length of the core trajectory, the radius of the core area and the rainfall depth in the core area (Fig. 2.43). Two further parameters describe the relative decrease of rainfall depth with increasing distance from the core. The combination of these can produce the full scala of 'homogenous' to 'heterogeneous' types of rain. These parameters can be related to frictional forces forming thunderstorms or convective bands causing frontal circulation (Pielke, 2002):

$$I_d = I_0 * (1 - e^{-(f^{\rightarrow}/d)^{f^{\leftarrow}}})$$

where:
d is distance of a cell from the storm core (grid unit);
I_d is rain intensity of a cell at distance d from the core (mm.d^{-1});
I_0 is rain intensity at the core (mm.d^{-1});
$f^{\rightarrow}$ is spreading factor; and
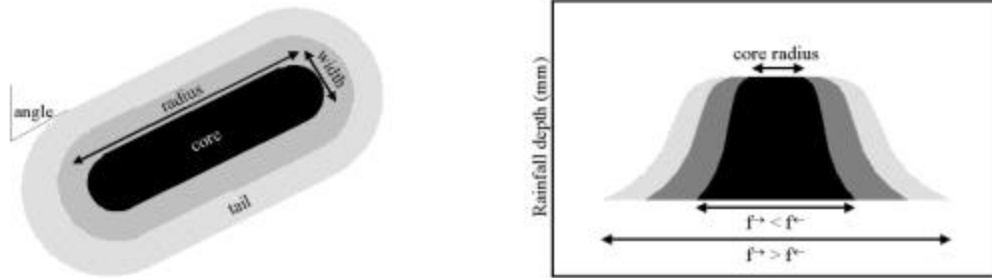$f^{\leftarrow}$ is agglomerating factor.

Figure 2.43. Assumed shape of individual storm events. Patchy rains are possibly formed when $f^{\rightarrow}$ < $f^{\leftarrow}$ (frictional forces), while homogenous rains are formed when $f^{\rightarrow}$ > $f^{\leftarrow}$ (frontal dynamics).

Matching spatial pattern with temporal pattern

A single storm event will 'wet' (above the measurement threshold of 0.5 mm day^{-1} used in most empirical data sets) a number of cells, some at the core intensity and some at a lower intensity. Given a set of parameters for the storm trajectory, we can derive the frequency distribution of rain depth in wetted cells, relative to the core rain intensity (p), in n classes. Once this is known, the frequency distribution of core intensities (F) can be

derived from the observed station level rain intensities (f). Frequency distributions of f, p and F should have the same class number and interval order. We use the following order to define the class boundary: [max..max*q^1],[max*q^1.. max*q^2], [max*q^2.. max*q^3],…,[max*q^n.. min], where max is the maximum data, min is the minimum data and n is class intervals number. The value of q is ranging from 0 to 1 and calculated as follows:

$$q = e^{\ln(\min/\max)/n}, q = 0\ldots1$$

We first need to recognize the combinations of classes p_j and F_k that are compatible with class f_i:

$$f_i = \sum_{j,k,i} \left(p_j F_k \mid j \& k \sim i \right); 0 \le f_i \le 1, 0 \le p_j \le 1, 0 \le F_k \le 1$$

For the highest rainfall class only one combination, involving the highest class of both p and F will yield the desired result, but for the other classes there can be several combinations of p and F that yield the same result (the tail end of a big rainfall event, a medium fraction of a medium storm or the core area of a small storm). We can approach it working our way from the top down, but a simpler derivation starts from the observation that for all distributions f, p and F the sum equals 1. By assuming that the resultant (f) comes from the multiplication between p and F, we then get this basic equation:

$$\sum_{i=1}^{n} f_i = \sum_{j=1}^{n} p_j * \sum_{k=1}^{n} F_k$$

So that F of frequency class n can be defined as:

$$F_n = \frac{\sum_{i=1}^{n} f_i}{\sum_{j=1}^{n} p_j} - \sum_{k=1}^{n-1} F_k$$

From the equation, we can derive a criterion for the shape of the p distribution (that depends on assumed storm properties) that is compatible with the targeted f distribution.

If at any point $\dfrac{\sum_{i=1}^{n} f_i}{\sum_{j=1}^{n} p_j}$ is less than $\sum_{k=1}^{n-1} F_k$, F_n would violate the assumption of non-negative

subsequent F terms. So, a cross-over of p and f indicates incompatibility of the storm-level assumptions — that generate the p curve — with the station-level rainfall records — that generate the f curve. Figure 2.44 illustrates the compatibility of intensity distribution from two contrasting spatial patterns of 30-grid maps with temporal distribution from 30-day station record. Pattern B of exactly similar distribution to the

station record rainfall produces compatible F as shown in Fig. 2.44.D, whereas pattern C is incompatible with the station record distribution as indicated by negative values of F in Fig. 2.44.E. This means, it is impossible to arrange rainfall maps of pattern C using the existing temporal distribution.
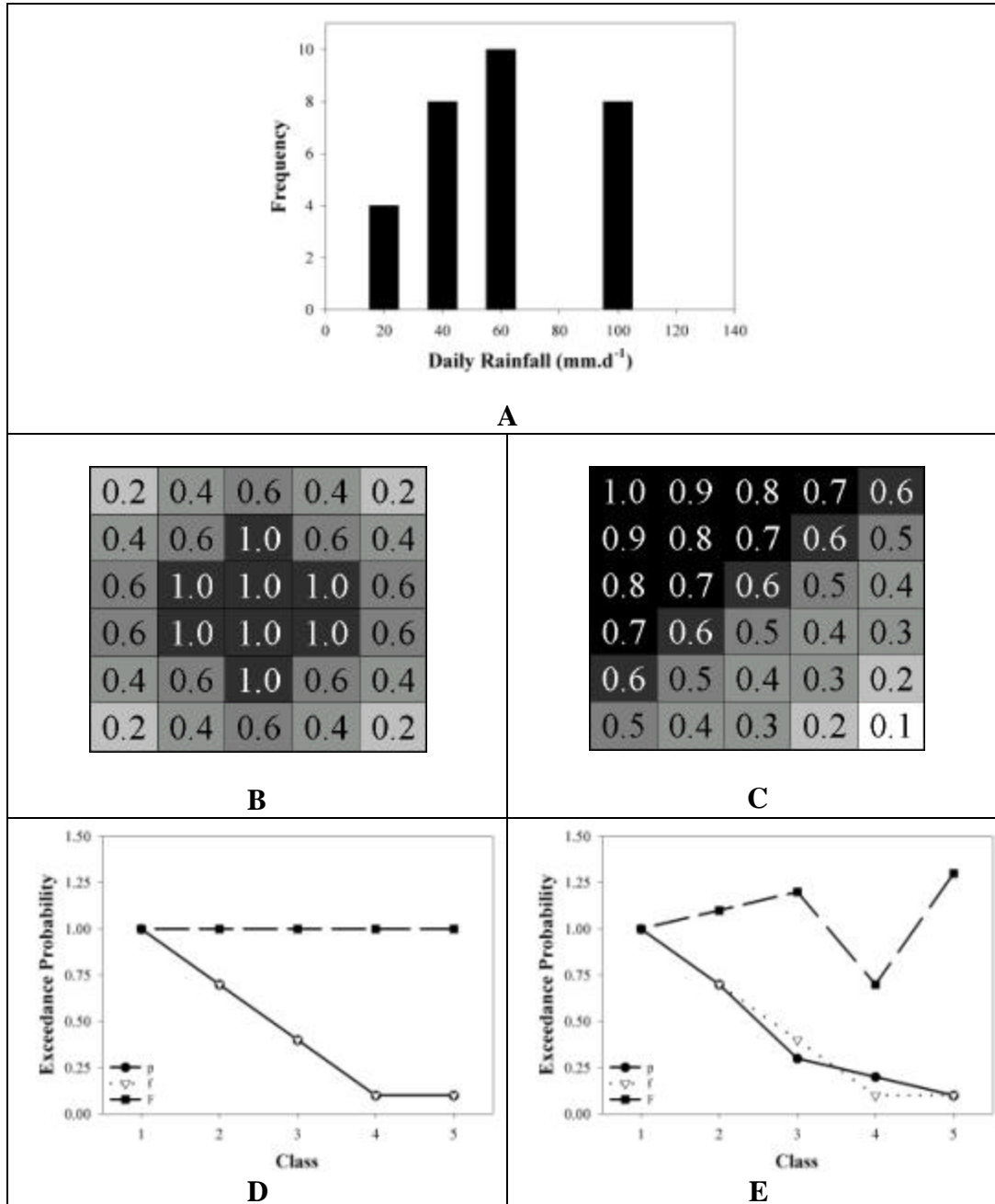

Figure 2.44. Compatibility of intensity distribution from two spatial patterns (B and C) with temporal distribution from station records (A). Pattern B is compatible (D) while pattern C is incompatible (E).

Considering multiple storm events

Equation $I_d = I_0 * (1 - e^{-(f^{\rightarrow}/d)^{f^{\leftarrow}}})$ may produce a narrow-spread area of single storm events, on which its wet cells ratio relative to total area (c_1) does not match the wet days fraction of that specific month (d).   Hence, we need to allow for multiple storm events, depending on the area fraction wetted by a single event and the time fraction of rainy days at the measurement station level. For spatially independent multiple events on a single day we can derive that probability of dry days on a given month, $P|\delta|$, should meet the probability of dry cells during single event, $P|\chi|$, to the power of events number (N):

$$P|\ddot{a}| = P|\div|^N$$

Where $P|\delta|=1-d$ and $P|\chi|=1-c_1.$ Thus, the number of events is:

$$N = \frac{\ln(1-d)}{\ln(1-c_1)}$$

Cross-scale probability of storm events

Patchy rains have less wet fraction than homogeneous rains in space. In order to conserve each cell to having uniform chance of being hit by storms in time, patchy rains should have higher probability to occur than homogeneous rains. Consequently, the cross-scale probability of storm with N number of events ($P(E_N)$) is defined from wet days fraction (d) by taking wet cells fraction of N storm events (c_N) into account:

$$P(E_N) = \frac{d}{c_N}$$

Considering elevational effect

Rainfall patchiness can also be affected by elevational effects of the area. Thus, rainfalls at particular degree of patchiness generated by the above procedures should be corrected if applied on an area with elevational effects. The elevation modifier of rainfall at elevation z (X_z) is assumed as rainfall average at that elevation (μ_z) relative to overall average (μ):

$$X_z = \frac{\grave{\imath}_z}{\grave{\imath}}$$

In fact we are modifying the amount of rain that any storm brings to any cell, not the preferred pathway of storm trajectories. Though similar multipliers we can introduce 'rain shadow' effects that depend on a preferential direction of storms and gradients in elevation.

Patchiness indicator

Semivariogram is used as quantitative spatial pattern indicator of simulated rainfall (Fig. 2.45). Spatial distribution of rain intensity from the storm cores can be distinguished by semivariance increase (dS) within the distance range of increasing semivariance (dh) or

the slope (s=dS/dh). From Fig. 2.45, it is expected that patchy rains will have higher dS within shorter dh (steeper slope) than homogeneous rains. Moreover, based on behavior of the slope, patchiness can be quantified using fractal dimension (D) (Bian,1997):
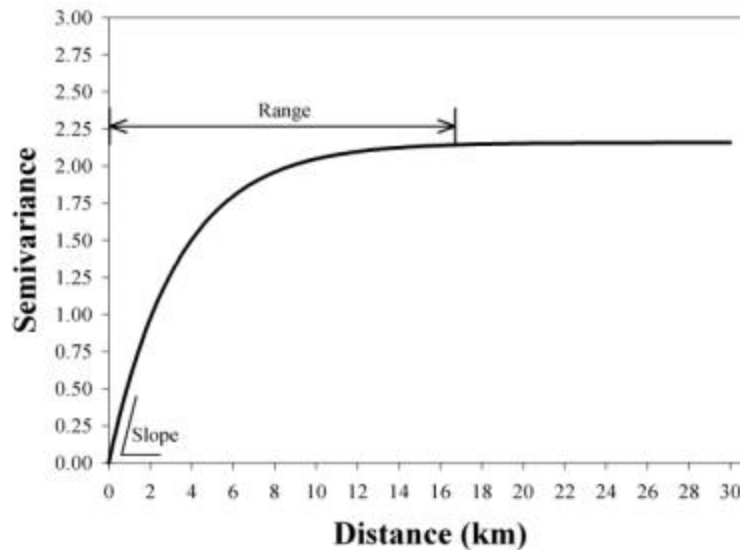
$$D = 3 - (s/2)$$

Figure 2.45. Fractal dimension as defined by slope of semivariance range is used as patchiness indicator of rainfall.

The value of D ranges from 0 to 3. Lower fractal dimension of a spatial pattern may be interpreted as more fragmented pattern. Thus, patchy rain is expected to have lower D than the homogeneous.

Implementation in SpatRain

A flowchart of the program that implements the above conceptualization is shown in Fig. 2.46. The SpatRain simulator is freely available on our website (http://www.worldagroforestrycentre.org/sea/products/AFmodels/spatrain.htm). The current version of the program is developed using VB macro in an Excel workbook. Application to the Mae Chaem area at a 3 km^2 grid cell resolution proved to be at the edge of the program's capability. To overcome the memory limitations, a standalone version of SpatRain has been developed using Java programming language. Fig. 2.47 shows one of the SpatRain-Java environment features in displaying the dynamic maps (daily rainfall maps as the simulation outputs), static scalar maps (*e.g.* DEM) and static discrete maps (*e.g.* sub-catchments boundary) at better resolution of 1 km^2 grid cell.
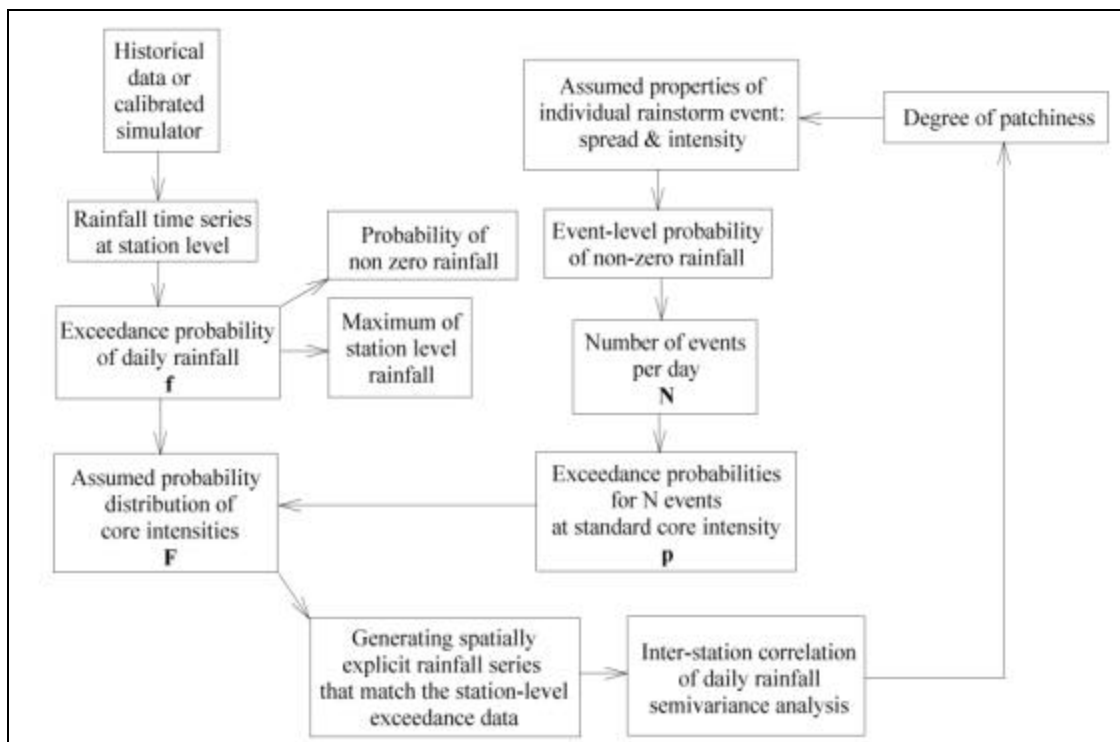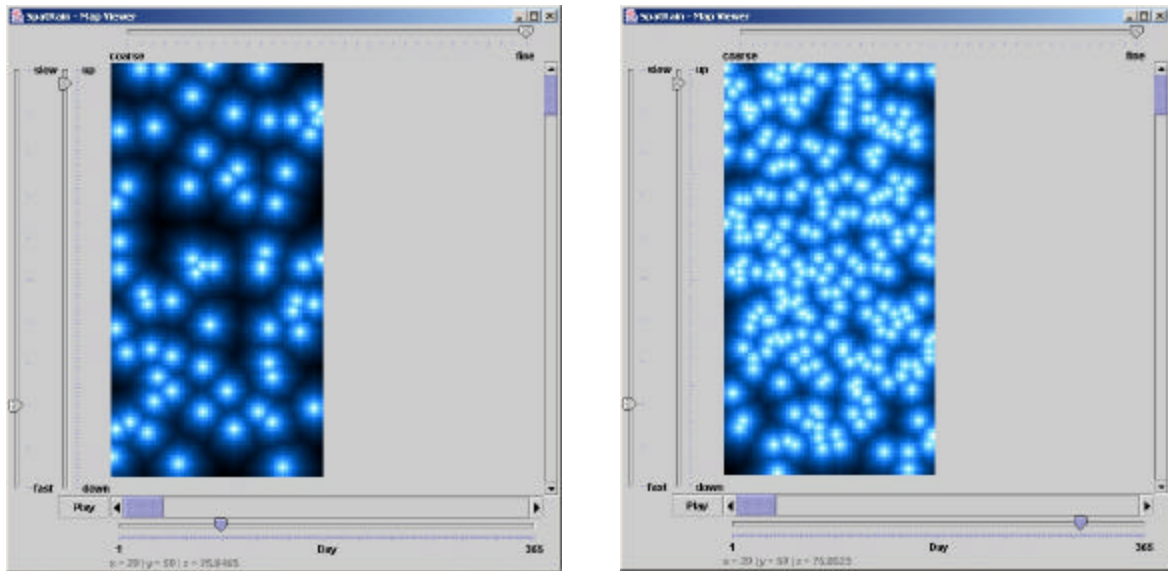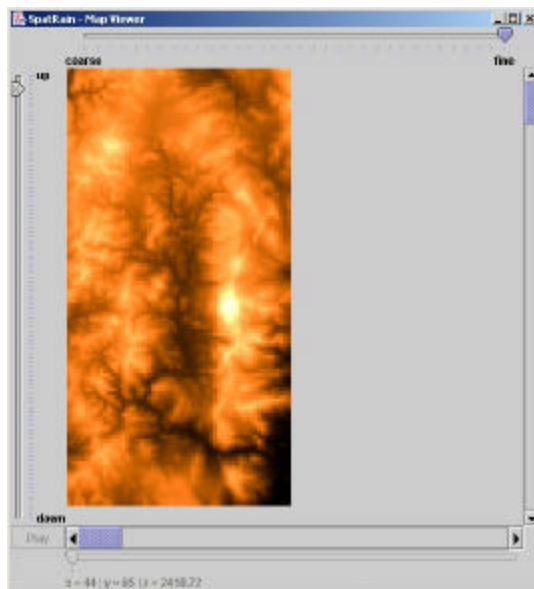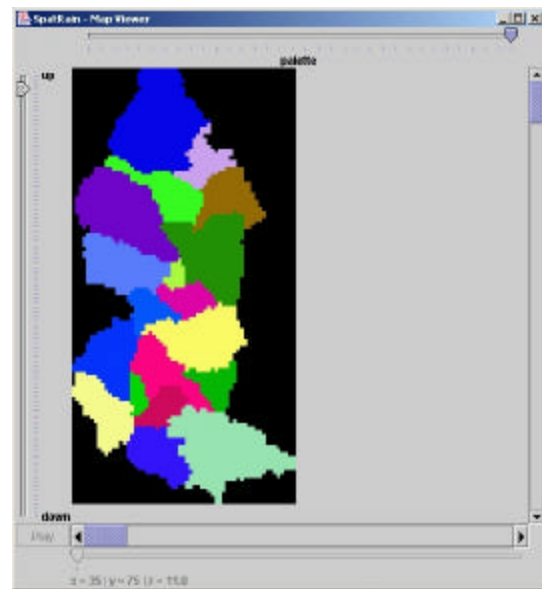
Figure 2.46. Flow diagram of model calculations in SpatRain

(A) Simulated Daily Rainfall Maps

(B) DEM

(C) Sub-cathment Boundary Map

Figure 2.47. SpatRain-Java capability in handling maps with large number of grids: (A) dynamic maps; (B) static scalar map (C) static discrete map.

2.2.6 WaNuLCAS

For a number of simulations reported here we made use of the detailed ('level 3) water of tree-soil-crop interactions WaNuLCAS (Van Noordwijk and Lusiana, 2000). The WaNuLCAS model was developed to simulate a range of tree–soil–crop interactions in agroforestry systems, for a wide range of soil, climate and slope conditions. Basic ecological principles and processes are incorporated into the model using modules such

as climate, soil erosion, sedimentation, water and nutrient balance, tree growth and uptake, competition for water and nutrients, root growth, and soil organic matter and light capture.

Where most models operating at landscape scale need information about infiltration, they are not able to describe this important process at the relevant time-scale. As there is important variation between soils in infiltration rates and there is no direct way to derive such information at the scale required for our models, we need estimation procedures, or 'pedotransfer' functions (Fig. 2.48).

INPUT

Percentage of clay	40	
Percentage of silt	10	
Percentage of organic matter (1.7*C-Organic)	4.08	
Median particle size of sand	290	
Top Soil ? (Type 1 for top soil, 0 for sub soil)	1	
Suggested value for Bulk Density	1.217	
Bulk Density	1.22	
K used for defining field capacity	0.1	**cm d-1**
Use the pedotransfer estimate of Ksat? 1 = yes, 0 = no	1	
Your own estimate of Ksat	110	**cm d-1**

Results

		m3 water m-3
Theta sat (Total saturated porosity)	0.485	soil
Ksat (saturated conductivity)	103.67	cm d-1
Alpha	0.0549	cm-1
Lambda	-3.737	
N	1.138	
		m3 water m-3
Field capacity based on critical K value	0.391	soil

Figure 2.48 A WaNuLCAS includes a pedotransfer function for estimating soil physical properties on the basis of soil texture, based on Wosten et al. (1995)

Field capacity can be defined on the basis of height above a water table (and hence read from the Theta - p relationship, or on the basis of a limiting unsaturated hydraulic conductivity. A model user is asked to specify the value you want to use for this second way of calculating where drainage effectively stops, e.g. 0.01 cm day-1. Inside WaNuLCAS the first way of calculating field capacity will be applied, and the highest value for theta from these two approaches will be applied in practice.
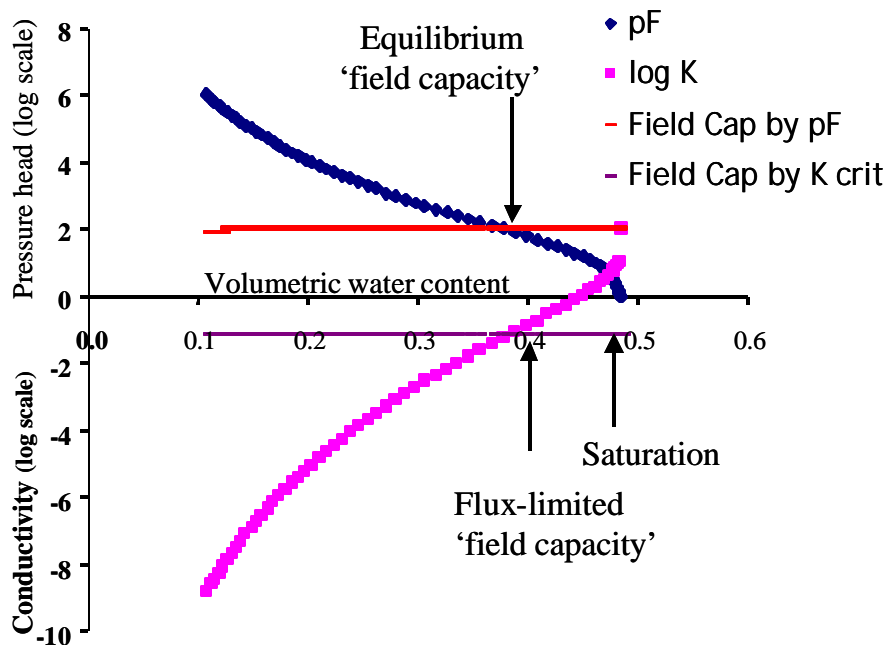
Figure 2.48 B Relationship between volumetric water content (θ), (negative) pressure head (h) and hydraulic conductivity (K) of a soil, as derived from the pedotransfer function used in WaNuLCAS from soil textural information and applied in the daily calculations of water transport in the soil

We will present a number of results regarding
   A) validity tests of the model for prediction of plot-level run-off and subsurface flows
   B) exploration of the pedotransfer functions used in WaNuLCAS
   C) analysis of surface runoff and erosion on the basis of rainfall intensity and soil structure
   D) analysis of changes in soil structure in a forest – coffee conversion time-series
   E) parametrizatrion of water balance for an intensification series of upland rice/fallow rotations in northern Thailand

A) validity tests of the model for prediction of plot-level run-off and subsurface flows

The subsurface lateral flow description in WaNuLCAS is based on a 2-dimensional extension of the "bucket overflow" concept. We decided to test the result of this with those for a more detailed continuous flow, finite element model such as FUSSIM. FUSSIM is a two-dimensional simulation model for describing water movement, solute transport and root uptake of water and nutrients in partially saturated porous media (Heinen and de Willigen, 1998).

The effect of slope and soil texture on lateral flow prediction according to WaNuLCAS and FUSSIM was simulated using rainfall data of Pakuan Ratu, Lampung, Indonesia for 1997, with a total rainfall of 1885 mm per year. In this exercise both model simulates a bare plot, 50 m in length and 2 m soil depth in sloping land. Slope was varied

between 15 – 90% and clay content was varied between 10 – 90%, keeping silt constant at 10%. At each run, the soil texture is homogenous over the whole soil layers.

B) exploration of the pedotransfer functions used in WaNuLCAS

Dynamic models of the soil-plant-atmosphere continuum can help to clarify relationships between land use and water resources, provided that they are correctly parameterized. The WaNuLCAS model for Water, Nutrient, and Light Capture in Agroforestry Systems was developed for such tasks in tropical conditions. However, the field measurements required for full model parameterization are laborious, costly and time consuming, so shortcuts are desirable. Pedo transfer functions (PTF) have been developed to predict the main soil physical relationships (θ-h-K) from the measured percentages of clay, silt, organic matter content, and bulk density. However, existing equations are largely based on temperate soils and as they are empirical, rather than based on first principles, these PTF's may gave erroneous, or even completely absurd predictions when used outside the range of soils from whose data they were derived. Even so, complete textural data are not easily obtained, and as a further step, these data themselves may be derived from soil classification data and manually assessed texture classes.

Suprayogo et al. (2003) described a new database, $P_{TF}RD_B$, of input parameters for PTF's derived from 8915 data available worldwide, with good representation of tropical soils. When the resultant estimates are used as basis for θ-h-K relationships, the results of the $P_{TF}RD_B$ appeared close to those derived from field measurements. The largest deviations occurred on vertisols and mollisols, where bulk density and soil organic matter content diverged.

A further test of these pedotransfer database was made for a 10 year simulation with WaNuLCAS for a simple agroforestry system. Total water use by trees and crop, as well as deep infiltration into the soil, surface and subsurface lateral flows were compared between a run based on full information on soil texture and bulk density, and runs based on coarser estimates and soil classes.

C) Linking surface runoff and erosion to rainfall intensity and soil structure

In WaNuLCAS, physical soil properties (i.e. texture, bulk density and organic matter content) and soil structure dynamics (i.e. biological activity, dependent upon nutrition provided by plants through litterfall and root decay) determine saturated hydraulic conductivity (K_{sat}), and condition the processes of lateral flow and vertical infiltration. Rain intensity, plant growth (through the interception of rain) and lateral flow (over the surface and as sub-surface flows) influence infiltration, which determines the amount of runoff water. Soil erosion is influenced by the amount of runoff water, the flow velocity (which determines the maximum transport capacity for particulate matter) and the actual concentrations of sediment (which depends on the particles' 'entrainment' or 'propensity to join the flow'). Actual sediment concentrations in overland flow thus depend on the steepness of the slope (determining the runoff velocity), the soil's surface cover (canopy of trees, shrubs, weeds, and litter: all of which reduce flow velocity at the surface and thus cause the sedimentation of particulate matter) and the coefficient of entrainment (which mainly depends on aggregate stability at the soil's surface).
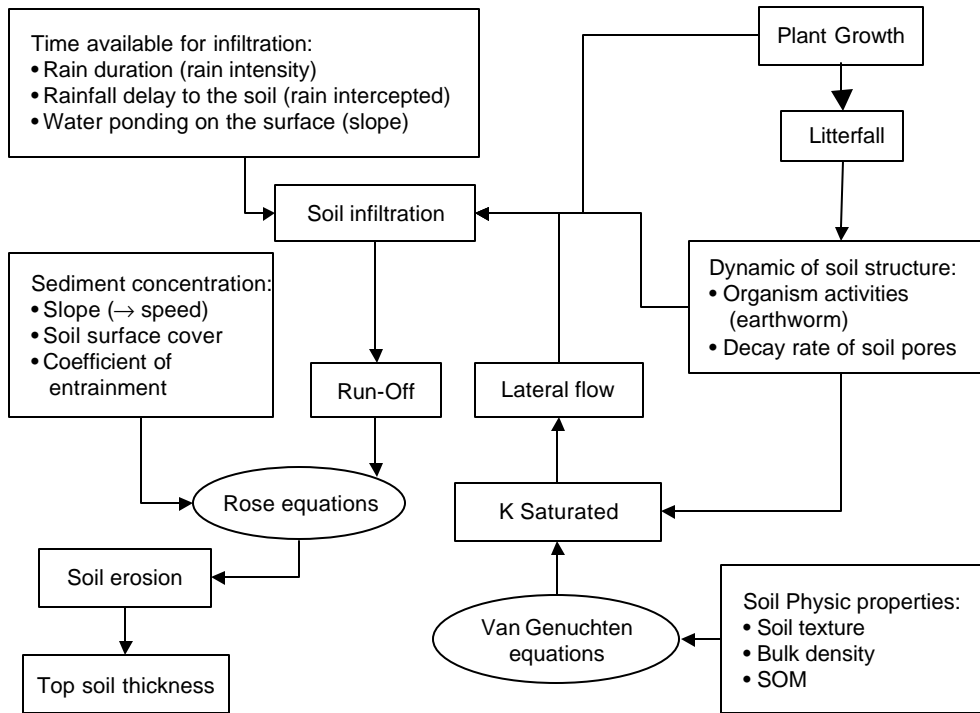
Figure 2.49. Key factors in the soil erosion component of the WaNuLCAS model, which include such well-established process descriptions as the 'van Genuchten' functions for soil water conductivity under saturated (K_{sat}) and unsaturated conditions, and the 'Rose equations' for overland flow of soil particles

Table 2.3. Soil infiltration rates for soils with good structure (Brouwer, *et al.*, 2000)

Soil texture	Infiltration rate, mm hr^{-1}	Infiltration rate, mm day^{-1}
Sand	> 30	>720
Sandy loam	20 - 30	480 – 720
Loam	10 - 20	240 – 480
Clay loam	5 - 10	120 – 240
Clay	1 - 5	24 – 120

Soil loss is based on an equation developed by Rose (1985):

$$E = 2700 * S * (1 - Cover) * \lambda * \frac{Q}{100}$$

with

E = soil loss per event (Mg ha^{-1})

S = sinus(slope)

Cover = fraction of soil-contact cover (0 – 1)

Q = surface runoff, mm per event

λ = entrailment factor with $\lambda = \lambda_{bare} e^{-0.15 Cover}$ and λ_{bare} = entrailment for bare soil

We compared simulations with an empirical data set based on runoff study in coffee gardens with ages of 0 – 10 years in Sumber Jaya, West Lampung, Indonesia

D) Dynamics of soil structure

WaNuLCAS uses a dynamic representation of soil structure that affects the saturated hydraulic conductivity and potential infiltration rate for the soil surface. The conductivity derived by the pedotransfer function for the 'default' soil bulk density (which reflect a large database for mainly European agricultural soils at 'standard' soil structure) is used as 'fall-back' value. The model user can specify a better starting point for soil structure (lower bulk density), but during the simulation there will be a decay of this additional structure, as well as an opportunity to build new macroporosity through biological effects based on the presence of surface litter.
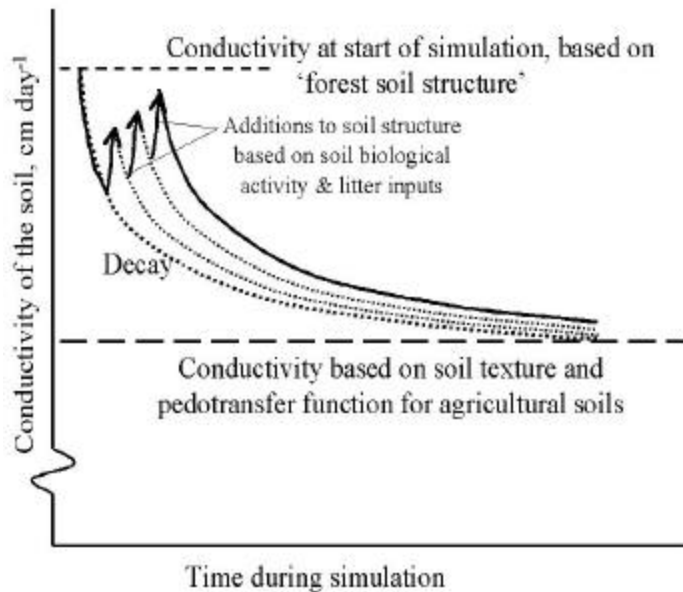

Figure 2.50. Schematic representation of the dynamics of soil structure as used in the WaNuLCAS model

E) Fallow intensification series for northern Thailand

The WaNuLCAS model of tree-soil-crop interactions was used as a tool to simulate crop yields, nutrient and water balance, in a series of 'scenarios' that represent reduced-fallow shifting cultivation systems. WaNuLCAS can be used for both sequential and simultaneous forms of agroforestry, and includes a module for 'slash-and-burn' land clearing. Simulations were set up for a 12-year test period that could be used for 11 years of fallow + 1 year of crop (growing upland rice), 10 years of fallow + 2 years of crop, 2 cycles of 5 or 4 year fallow and 1 or 2 years crop, or 3 cycles of 1, 2 or 3 years of fallow plus 3, 2 or 1 years of crop. Soil property data were derived from Wangpakapattanawong (2001) and from default values of the model. The tree parameters were derived from the default values for *Peltophorum* in the WaNuLCAS tree library. Whenever the land was not cropped, annual weeds were allowed to grow, using parameters for an 'annual' weed that would die back at maturation and regrow from a seedbank.

2.2.7. VIC (The Mekong Basin)

Streamflow regulation, deforestation, agricultural expansion and other man made changes taking place in the Mekong basin have the potential to affect the streamflow patterns of the Mekong and its tributaries and could have serious environmental, economic, and social impacts on the region. The response of the Mekong water resources system to these changes can be viewed as an interaction between the land surface hydrologic cycle, the physical infrastructure of the water resources system (dams and reservoirs), and water resources management practices (reservoir operating policies). Our intent is to examine the underlying dynamics of he hydrologic cycle in the Mekong, and to use that understanding in an attempt to under and ultimately predict the response of the system to change.

The work being executed here is predicted on the ability to dynamically describe the movement of water in drainage basins, from its mobilization across the landscape to small streams, and subsequently down the channel system to large rivers. The methodology chosen is to utilize a set of coupled geospatial models of the physical aspects of the landscape with hydrology models, and the dataframes required to support them. Hydrologic and water management simulation tools can be used to explore the response of the water resources system to these interactions. Macro-scale hydrology models can simulate rainfall-runoff processes of large river basins like the Mekong (Nijssen et al., 1997). These models are designed to represent the effects of vegetation on runoff, and thus can be used to simulate the effects of vegetation change (like deforestation and agricultural expansion) on surface hydrological processes. The effects of flow regulation can be simulated using water management models (Hamlet and Lettenmaier, 1999; Leung et al., 1999). Thus, a hydrology model when combined with a water management model (e.g. Hamlet and Lettenmaier, 1999) can be used to model the streamflow of the Mekong River and its tributaries.

It is worth noting that this basic strategy goes beyond "just" analysis of hydrographs.
1. Being able to even assemble the requisite data sets is already an important synthetic activity. These data sets are very rarely complete (or even close to it); hence models can be used as interpolation devices, allowing a more complete analysis. Assembly of even what is considered "dataframes" or GIS layers actually represents important decisions; where each such "layer" is a data model in its own right.
2. If a model gets the variability in a time series about "right" (without force fitting), then understanding is implicit.
3. The model can then be used to decompose the hydrograph signal into its constituent processes.
4. With such a dynamical base, scenarios can be explored with some confidence.

2.2.7.1. VIC: The Hydrology Model

We based our analysis of the dynamics of water movement across the Mekong basin on the Variable Infiltration Capacity (VIC) model, coupled to water routing and water management models.

VIC (Liang *et al*, 1994) was specifically designed for analysis of water (and energy) fluxes in regional-scale, large river basins. It is a physically based model, which nonetheless parameterizes small scale processes to allow application to large river basins, which typically are resolved at spatial resolutions from 1/8 degree latitude by longitude (e.g., where the resolution of the precipitation, temperature, radiative, and other surface forcings are available or can be derived) to coarser resolutions such as the 2 degree global application described by Nijssen *et al* (2002). Previous applications of VIC include such large continental river basins as the Columbia (Nijssen et al., 1997), the Arkansas-Red (Abdulla et al., 1996), and the Upper Mississippi (Cherkauer and Lettenmaier, 1999), among other rivers. VIC has also been applied to the entire area of China (Su and Xie, 2003).

a) Surface Water and Energy Balance over a grid cell. A detailed description of the VIC model can be found in Liang et al. (1994, 1996 and 1998) and Nijssen et al. (1997). Briefly, the model (Fig. 2.51) has parameterizations to represent the vertical exchange of moisture and energy between the vegetation canopy and the atmosphere, similar in many respects to other Soil-Vegetation-Atmosphere Transfer Schemes (SVATS). Its main distinction from other SVATS is its representation of the effects of sub-grid spatial variability in soil, topography, and vegetation (each vegetation cover class occupies a specified fraction of the grid cell, as shown in the figure), and their effects on runoff generation. VIC also simulates the spatial sub-grid variability in precipitation: the area fraction of the grid cell experiencing precipitation increases with increasing intensity of the precipitation event (Liang et al., 1996). For each vegetation cover class, the leaf area index (LAI), canopy resistance, and relative fraction of roots in each soil layer is specified. Evapo-transpiration from each vegetation type is calculated using a Penman-Monteith formulation (Liang et al., 1994).
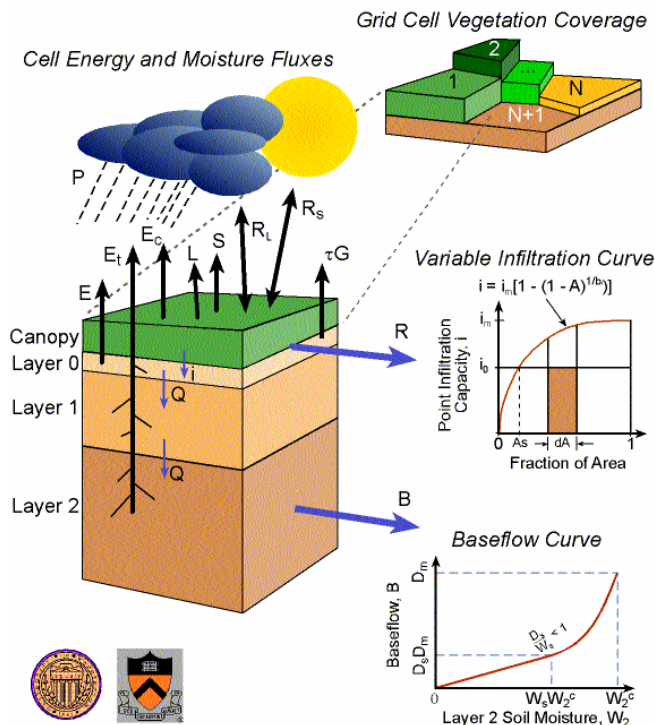

Figure 2.51. Variable Infiltration Capacity - nLayer (VIC-nL) macroscale hydrologic model

The soil is divided in the vertical direction in an arbitrary specified number of layers (for most applications, 2 or 3 layers are commonly used). The sub-grid horizontal variability in soil properties is represented statistically, using a spatially varying infiltration capacity. The variable infiltration curve (shown in the figure) represents the fraction of the grid cell where fast runoff is produced (by either saturation excess, or fast sub-surface flow). Drainage between the soil layers is modeled as gravity driven, and the unsaturated hydraulic conductivity is a function of soil moisture content, following the parameterization by Campbell (1974). Another distinguishing characteristic of VIC is the representation of base flow from the deeper soil layer as a nonlinear recession, following the ARNO model base flow formulation (Todini, 1996).

The VIC model can be operated in two different modes: an energy balance mode and a water balance mode. In the energy balance mode, all the water and energy fluxes near the land surface are calculated, and the surface energy budget is closed by iterating over an effective surface temperature. In the water balance mode, the effective surface temperature is assumed to equal the air temperature and only the surface water balance fluxes are calculated. In this study, the VIC model is operated in the water balance mode, which is equivalent to the manner in which most operational hydrological models function. Precipitation, maximum and minimum temperature, and wind speed are the meteorological variables that drive the model in the water balance mode. Hourly temperatures are estimated by fitting a spline function to the time series of daily minimum and maximum temperatures. Daily precipitation inputs are distributed uniformly in time throughout the day.
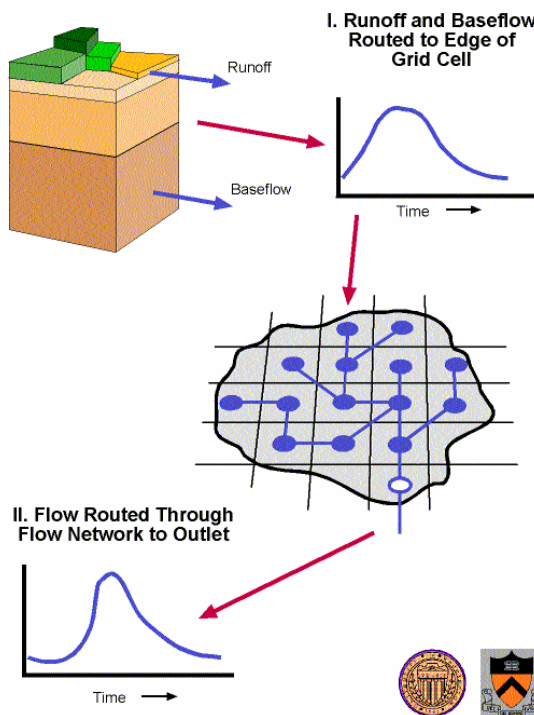

Figure 2.52. River network routing scheme for VIC-nL

b) *Streamflow Routing*. The VIC model is coupled to a streamflow routing scheme (Fig. 2.52) that transports the runoff generated within each grid cell through a specified channel network. The scheme (Lohmann et al., 1996 and 1998) uses linearized St. Venant's equations, and permits computation of the hydrograph at any point of interested in the channel network. The single runoff time-series produced for each grid cell is routed to the grid cell outlet using a triangular unit hydrograph. Flow from each grid cell can exit into any one its eight neighbors. The routing model does not account for water management (channel losses, extractions, diversions and reservoir operations).

c) *Water Management: Reservoir Water management and Irrigation*. Water resources currently sustain a relatively dense population of 73 million people who obtain most of their protein from fish harvested from the river. Many people also rely heavily on the annual flooding cycle for crop irrigation. The anthropogenic changes taking place in the Mekong Basin have significant implications on the resources of the Mekong River. Population growth in the Mekong Basin has resulted in widespread conversion of forests into agricultural uses to meet increased demand for food. The increase in agricultural areas and irrigation, along with urbanization and industrialization, led to an overall increase in demand for water. The major water infrastructures in the basin are the dams, which were constructed over the last four decades in China, Lao, Vietnam and Thailand. In Cambodia and Vietnam, the wetlands, Tonle Sap Lake and the numerous dykes form the main water infrastructures are playing a role directly or indirectly in the occurrence of the flood and also the drought in the basin. Massive hydroelectric dams are planned or have already been constructed along the river course.
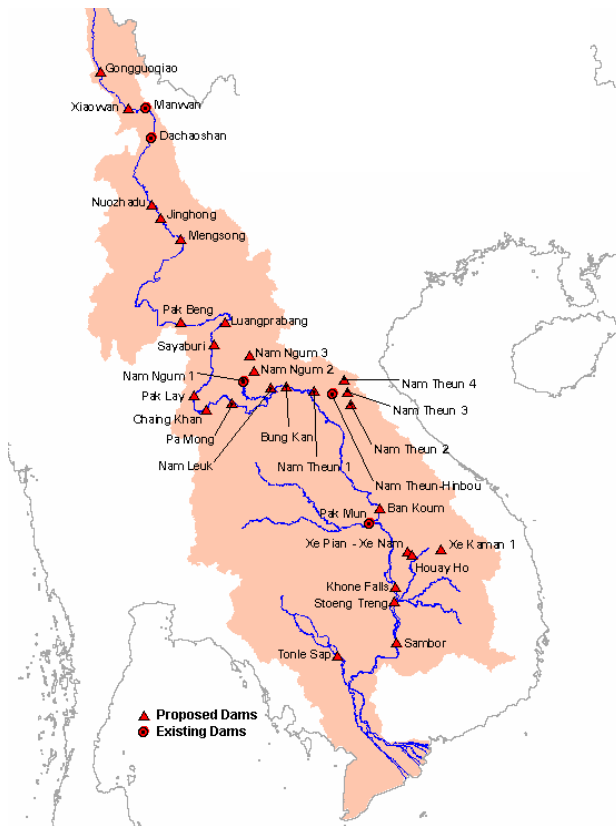

Figure 2.53. Existing and proposed dams in the Mekong Basin